Neuron, Volume *60*

Article

Bhlhb5 Regulates the Postmitotic Acquisition of Area Identities in Layers II-V of the Developing Neocortex

Pushkar S. Joshi, Bradley J. Molyneaux, Liang Feng, Xiaoling Xie, Jeffrey D. Macklis, Lin Gan

---

Supplemental Experimental Procedures

Generation of *Bhlhb5-Cre* Knock-in Mice

The *Bhlhb5-Cre* knock-in construct was generated by replacing the *Bhlhb5* coding region with nuclear *Cre recombinase* coding region. The construct fuses *Cre* immediately upstream of the Bhlhb5 translation initiation codon in the 5'-untranslated region, and places *Cre* under the transcriptional control of *Bhlhb5* regulatory sequences. To generate *Bhlhb5*-Cre knock-in mice, the AscI linearized *Bhlhb5-Cre* construct was electroporated into W4 embryonic stem cells (a gift from A. Joyner, New York University), and three targeted clones were obtained by drug selection with G418 and FIAU, and Southern blotting genotyping. Two targeted ES cell clones were injected into C57BL/6J blastocysts to generate mouse chimeras. Heterozygous *Bhlhb5*$^{cre/+}$ mice were generated in 129S6 and C57BL/6J mixed background as described (Gan et al., 1999; Gan et al., 1996). The PCR primers used to identify *Cre* knock-in allele were 5'-GGGATTGGACTCAGAGGCGGTAGC-3' and 5'-GCCCAAATGTTGCTGGATAT-3'. The primers used to identify *Bhlhb5* wild-type and *lacZ* knock-in alleles were previously described (Feng et al., 2006).

Immunocytochemistry, In Situ Hybridization and X-Gal Staining

Decapitated heads (E12.5-E17.5) or brains (P0-P7) were drop fixed in 4% paraformaldehyde (PFA) for 24-48 hours at 4°C. Mice beyond P7 were transcardially perfused with 4% PFA followed by 12 hours of post-fixation at 4°C. Brains were either sectioned on a vibratome at 50 µm or equilibrated in 30% sucrose, frozen in OCT medium (Tissue-Tek), and cryosectioned between 20-50 µm. Sections thicker than 30 µm were processed free floating.

BrdU was injected into pregnant dams at 75mg/kg bodyweight for 30 minutes, and embryos were then isolated. For immunocytochemistry, the following antibodies were used: goat anti-Bhlhb5 (1:300, Santa Cruz); mouse anti-bromodeoxyuridine (BrdU) (1:50, Developmental Studies Hybridoma Bank); rabbit anti-Phospho-Histone 3 (PH3) (1:400, Santa Cruz); mouse anti-Ki67 (1:300, BD Pharmingen); rabbit anti-ß-tubulin (Neuronal Class III; Tuj1) (1:300, Covance); rabbit anti-glutamate (1:1000; Sigma); rabbit anti-GABA (1:1000, Sigma); rat anti-CTIP2 (1:300, Abcam); rabbit anti-Tbr1 (1:500, a gift of R.Hevner); rabbit anti-SERT (1:500, Immunostar); rabbit anti-PKCγ (1:500, Santa Cruz); chicken anti-GFP (1:500, Abcam); and rabbit anti-GFP (1:500, MBL). The following secondary antibodies were used: biotinylated goat and rabbit (Vector); Donkey anti-rat Cy3 (Jackson Immunoresearch); and Alexa antibodies (Molecular Probes). Fluorescent images were captured by a digital camera using an Olympus or Biorad confocal microscope or a Zeiss Axioplan or Nikon E1000 microscope.

Non-radioactive *in situ* hybridization was performed on 20-35 µm thick sections. The following probes were used: *Bhlhb5* (3'UTR of NM_021560)*; Cad8* (241-1481 of X95600)*; RORß* (1573-2087 of NM_146095)*; Brn2* (849-1296 of NM_008899)*; COUP-TF1* (gift of M. Tsai)*; Pax6* (gift of X. Zhang)*; Lmo4* (gift of T. Rabbitts)*; Er81* (gift of S. McConnell)*; Tbr1* (gift of R. Hevner)*; Etv5* (The I.M.A.G.E.

Consortium, GenBank number BF021513); *EphA7* (gift of T. Mori)*; ephrin-A5; Id2; Emx2* (gift of J. Rubenstein); *p75* (gift of K-F. Lee); *Ten_m3* (gift of C. Leamey)*; S100A10; Mu-crystallin; Crim1; Cux2* (Arlotta et al., 2005; Molyneaux et al., 2005). Images were converted into negatives using Adobe Photoshop.

For X-Gal staining, whole mount brains were fixed in 4% paraformaldehyde between 2-6 hours at 4°C and incubated for 24-36 hours at room temperature with 0.1% X-Gal, 2 mM $MgCl_2$, 5 mM potassium ferricyanide, and 5 mM potassium ferrocyanide in PBS. Brains were fixed for 10 hours when X-Gal staining was performed on sections.

Cortical Map and Barrel Cortex Analysis

To visualize the sensory map, X-Gal reactions were performed on P6 *Bhlhb5*$^{lacZ/+}$ and *Bhlhb5*$^{lacZ/lacZ}$ whole mount brains for 24 and 3 hours respectively. Reactions of shorter duration, just enough to delineate area borders, were performed on *Bhlhb5*$^{lacZ/lacZ}$ brains, due to higher levels of Bhlhb5-lacZ compared with controls. The cortical map, including the PMBSF, was visualized either by cytochrome oxidase histochemistry, or by HRP immunohistochemistry for SERT on tangential cortical sections. Images of the cortex were obtained, and negatives were generated for better visualization for quantification. To visualize post-synaptic organization of barrels, SERT immunolabeled (fluorescent) sections were either counterstained with Nissl or Sytox Green nucleic acid stain (1:10,000, Invitrogen). Quantification of surface areas of cortical domains and primary areas were made using the UTHSCSA ImageTool software. GraphPad Prism was used for statistical analyses, including the Student's *t* test.

Whole Mount Analysis

For whole mount analysis of the cortex and pyramidal tract, mice were euthanized, and brains were dissected out and placed in cold PBS without fixation. Cortices were removed to observe the cerebral peduncle at P0. Images were immediately captured in white light or at 547 nm for DiI or 488nm (UV) for GFP visualization. Of note, the CST phenotypes observed in *Bhlhb5*$^{lacZ/cre}$*; Z/EG/+* nulls were verified in *Bhlhb5*$^{cre/cre}$*; Z/EG/+* nulls (data not shown).

Supplemental Figure Legends

Figure S1. Bhlhb5 Expression in the Forebrain.
(A) HRP-immunocytochemistry for Bhlhb5 in E15.5 dorsolateral telencephalon reveals strong Bhlhb5 expression in the CP, weak expression in the subventricular zone (SVZ), and no expression in the ventricular zone (VZ).
(B) Bhlhb5 does not colocalize with the proliferative cell marker Ki67 in the VZ or SVZ at E15.5.
(C) Bhlhb5 colocalizes with the post-mitotic neuronal marker Tuj1 in a subset of terminally migrated post-mitotic neurons in the CP, and in presumptive pre-migratory post-mitotic neurons in the SVZ at E15.5. (D-F) Magnified view of boxed area in the CP in (C). (G-I) Magnified view of boxed area in the SVZ in (C).
(J) Bhlhb5 is not expressed by GAD67-GFP expressing interneurons in the neocortex at P0. (K) Magnified view of boxed area in (J).
(L-N) Bhlhb5 is not expressed in medial (M) and caudal ganglionic eminences (C), the extracortical sites of dorsal telencephalic GABAergic interneurons, during peak production at E12.5-E13.5.
(O-T) Bhlhb5 is not expressed in any nucleus of the dorsal thalamus (dT) from E13.5 to P4, during generation and cortical axonal targeting of dorsal thalamic projection neurons. L, lateral ganglionic eminence; A, anterior; P, Posterior. Scale bars: 50µm (A,J), 25µm (B,C,K), 250 µm (L-O), 500 µm (P-T). (D-I) not to scale.

Figure S2. Generation of *Bhlhb5-lacZ* and *Bhlhb5-Cre* Knock-in Mice.
(A) *Bhlhb5* genomic structure, restriction enzyme map, and targeting strategy. The DNA fragment containing *Bhlhb5* open reading frame (ORF) region is replaced with reporter *ß-galactosidase (lacZ)* or *Cre-recombinase* gene in the targeting vector. Neo, PGK-neo gene cassette for positive selection; TK, MC1-TK gene cassette for negative selection. (B) Southern and PCR genotyping of litters from *Bhlhb5*$^{lacZ/+}$, and *Bhlhb5*$^{lacZ/+}$ or *Bhlhb5*$^{cre/+}$ heterozygote crosses. The 5'-Southern probe detects 8.1 kb wild-type and 5.1 kb mutant XbaI fragments. PCR genotyping primer sets generate 623 bp wild-type and 404 bp *lacZ* and 590 bp *cre* bands, respectively. (C) Anti-Bhlhb5 immunocytochemsitry reveals absence of

Bhlhb5 protein in P4 *Bhlhb5* null brain sections. (D) *Bhlhb5* nulls are smaller than their wild-type and heterozygous littermates by one month of age. Scale bar: 500 µm.

Figure S3. Normal Cell Survival and Lamination in *Bhlhb5 nulls*.
(A) X-Gal reaction on coronal sections along the rostrocaudal extent of P5 *Bhlhb5*$^{lacZ/+}$ (heterozygote control) and *Bhlhb5*$^{lacZ/lacZ}$ (*Bhlhb5* null) brains reveals normal survival and migration of an overwhelming majority of *Bhlhb5*-expressing neurons in *Bhlhb5* null cortex.
(B-G) *In situ* hybridization for (B) *Brn2* (layers II, III and V) (McEvilly et al., 2002; Sugitani et al., 2002), (C) *Cux2* (layers II-IV) (Nieto et al., 2004; Zimmer et al., 2004), (D) *Tbr1* (layer VI and subplate) (Hevner et al., 2001), (E) *Er81* (layer V) (Hevner et al., 2003), and immunocytochemistry for (F-H) CTIP2 (layer V CSMN and other SCPN) (Arlotta et al., 2005) on P5 *wild-type* and *Bhlhb5*$^{lacZ/lacZ}$ brain sections, reveals a morphologically normal cortex with six distinct layers in *Bhlhb5* nulls. White arrowheads in (G) point to a subtle compaction of layer V sub-layers in the caudal motor cortex of *Bhlhb5* nulls. (H) Magnified view of CTIP2 immunolabeled caudal motor cortex. There appear to be fewer CTIP2+ neurons in layer V (between green dashed lines) of *Bhlhb5* nulls (n=2; Mean±SEM=280±34 CTIP2+ neurons) than in layer V of *wild-types* (n=2; Mean±SEM=331±23 CTIP2+ neurons). However, the density of CTIP2+ neurons in *Bhlhb5* nulls (Mean±SEM=61.2±6.8 CTIP2+ neurons/mm^2) appears modestly increased compared to *wild-type* (Mean±SEM=51±0.24 CTIP2+ neurons/mm^2). (A-G) (*controls* n=3; *Bhlhb5* nulls n=3); S, sagittal; WM, white matter; Scale Bars: 1 mm.

Figure S4. Expression of *p75*, *Etv5*, and *Ten_m3* Is Unaltered in *Bhlhb5* null Mice.
In situ hybridization on P1 sagittal brain sections for (A) the neurotrophin receptor *p75*, expressed in a caudal to rostral gradient in layer VI and subplate, and (B) transcription factor *Etv5*, expressed in multiple layers of the rostral motor cortex, reveals normal expression patterns in *Bhlhb5* nulls. This demonstrates the specificity of Bhlhb5-mediated gene expression as Bhlhb5 lacks normal coincident expression with these two markers. (C) Despite normally coincident expression with Bhlhb5, *in situ* hybridization on P5 sagittal brain sections for *Ten_m3*, a type II transmembrane glycoprotein enriched in layer V corticotectal projection neurons of the occipital cortex (arrow) reveals unaltered expression. (*wild-types* n=3; *Bhlhb5* nulls n=3); Scale bars: 1mm.

Figure S5. Bhlhb5 Does Not Suppress Rostral Motor Identity in the Caudal Sensory Domain.
(A-C') Negative images of the cortical map revealed via (A,A') X-Gal reactions on whole mount P6 control (*Bhlhb5*$^{lacZ/+}$; n=6) and *Bhlhb5* null (*Bhlhb5*$^{lacZ/lacZ}$; n=5) brains; (B,B') HRP-immunohistochemistry for serotonin transporter (SERT) on tangential sections through P7 control (*wild-type*; n=7) and *Bhlhb5* null (*Bhlhb5*$^{lacZ/lacZ}$; n=7) cortices; and (C,C') cytochrome oxidase (CO) histochemistry on tangential sections through P7 control (*wild-type*; n=7) and *Bhlhb5* null (*Bhlhb5*$^{lacZ/lacZ}$; n=6) cortices.
(D) X-Gal reaction and SERT immunohistochemistry reveal an unaltered rostal motor (M) to sensory (S) domain surface area ratio in *Bhlhb5* nulls. This indicates that the rostral motor domain does not expand caudally at the expense of the sensory domain.
(E) Primary visual area (V1) to total cortical area (T) ratio reveals a 20% increase via X-Gal reaction and 14% increase via SERT immunohistochemistry in the proportional size of V1 in *Bhlhb5* nulls.
(F) Posteromedial barrel subfield (PMBSF or B) to total cortical area ratio reveals a 23% increase via cytochromoxidase histochemistry and a 26% increase via SERT immunohistochemistry in the proportional size of the PMBSF in *Bhlhb5* nulls.
(G-I) *In situ* hybridization for molecules that specify areal/positional identity in progenitors, (G) *Emx2*, (H) *Pax6*, and (I) *COUP-TF1*, reveals their unperturbed gradients in the cortical primordium of E13.5 *Bhlhb5* nulls (n=3/ group).
In (D-F), surface area ratios are plotted as mean±SD; * indicates $p<0.05$; *** indicates $p<0.0001$. Scale bars: 1 mm (A-C'), 500 µm (G-I).

Figure S6. Analysis of Bhlhb5 Expression in Retrogradely Labeled CSMN in Postnatal Caudal Motor Cortex.
(A) Schematic depicting retrograde FluoroGold (FG) labeling of the corticospinal tract (green arrowhead) to back-label CSMN in the *wild-type* cortex.
(B) Back-labeled FluoroGold+ CSMN in P6 caudal motor cortex section immunolabeled for Bhlhb5.

(C) Magnified view shows lack of Bhlhb5 expression in the majority of medial (M) CSMN in caudal motor cortex.
(D) Magnified view shows Bhlhb5 expression in a majority of lateral (L) CSMN in caudal motor cortex.
This medio-lateral difference in Bhlhb5 expression at P6 is likely due to mediolateral cortical downregulation of Bhlhb5 postnatally. Scale bar: 50 µm.

Figure S7. Genetic Lineage Tracing Confirms the Patterned Neocortical Expression of *Bhlhb5* and Reveals the Trajectory of *Bhlhb5*-expressing CSMN axons.
(A) Dorsal views of whole-mount P3 brains from *Z/EG* (negative control), *Bhlhb5*$^{cre/+}$*; Z/EG/+* and *CMV-cre Z/EG* (positive control) mice illuminated under white or UV light. In *Bhlhb5*$^{cre/+}$*; Z/EG/+* brains, Bhlhb5-Cre specifically triggers continuous GFP production in Bhlhb5 lineage cells, revealing high fluorescence in caudal sensory cortex and low fluorescence in rostral motor cortex. This correctly recapitulates Bhlhb5's cumulative patterned expression in the neocortex.
(B) Endogenous GFP fluorescence in side and ventral views of whole-mount P0 and P20 *Bhlhb5*$^{cre/+}$*; Z/EG/+* brains, respectively, reveals *Bhlhb5*-expressing axons in the cerebral peduncle (CPD) and PT (pyramidal tract).
(C) Diffusion of GFP reporter throughout the entire length of corticospinal axons is confirmed via immunohistochemical co-labeling of GFP with the corticospinal tract (CST) marker PKCγ, on P21 brainstem and spinal cord sections. D, pyramidal decussation; CB, cerebellum; Scale bars: 1 mm (A,B), 500 µm (C).

Figure S8. Regulation of Bhlhb5 Stoichiometry via Auto-feedback Inhibition.
(A,B) Despite one *Cre* copy in *Bhlhb5*$^{cre/+}$*; Z/EG/+* heterozygotes (n=6) and *Bhlhb5*$^{cre/lacZ}$*; Z/EG/+* nulls (n=17), dorsal views of whole mount brains reveal higher endogenous GFP fluorescence in *Bhlhb5* nulls.
(C,D) At P5, double immunolabeling reveals a greater number of GFP+ CTIP2+ subcerebral projection neurons in layer V of *Bhlhb5* nulls (n=3) than in heterozygotes (n=3).
(E) Overnight X-Gal reaction performed on whole mount P4 *Bhlhb5*$^{cre/lacZ}$ (one *lacZ* copy; n=3) null brain reveals reaction product greater than *Bhlhb5*$^{lacZ/+}$ heterozygote contro1 (one *lacZ* copy; n=3), and similar to *Bhlhb5*$^{lacZ/lacZ}$ null (two *lacZ* copies; n=3).
Taken together, these observations suggest that Bhlhb5 regulates its stoichiometry via auto-feedback inhibition, and that some of the GFP+ CSMN axons in the reduced pyramidal tract of *Bhlhb5* nulls might originate from CSMN that express normally undetectable levels of Bhlhb5 during development. Scale bars: 1 mm (A,C), 500 µm (B).

Figure S1

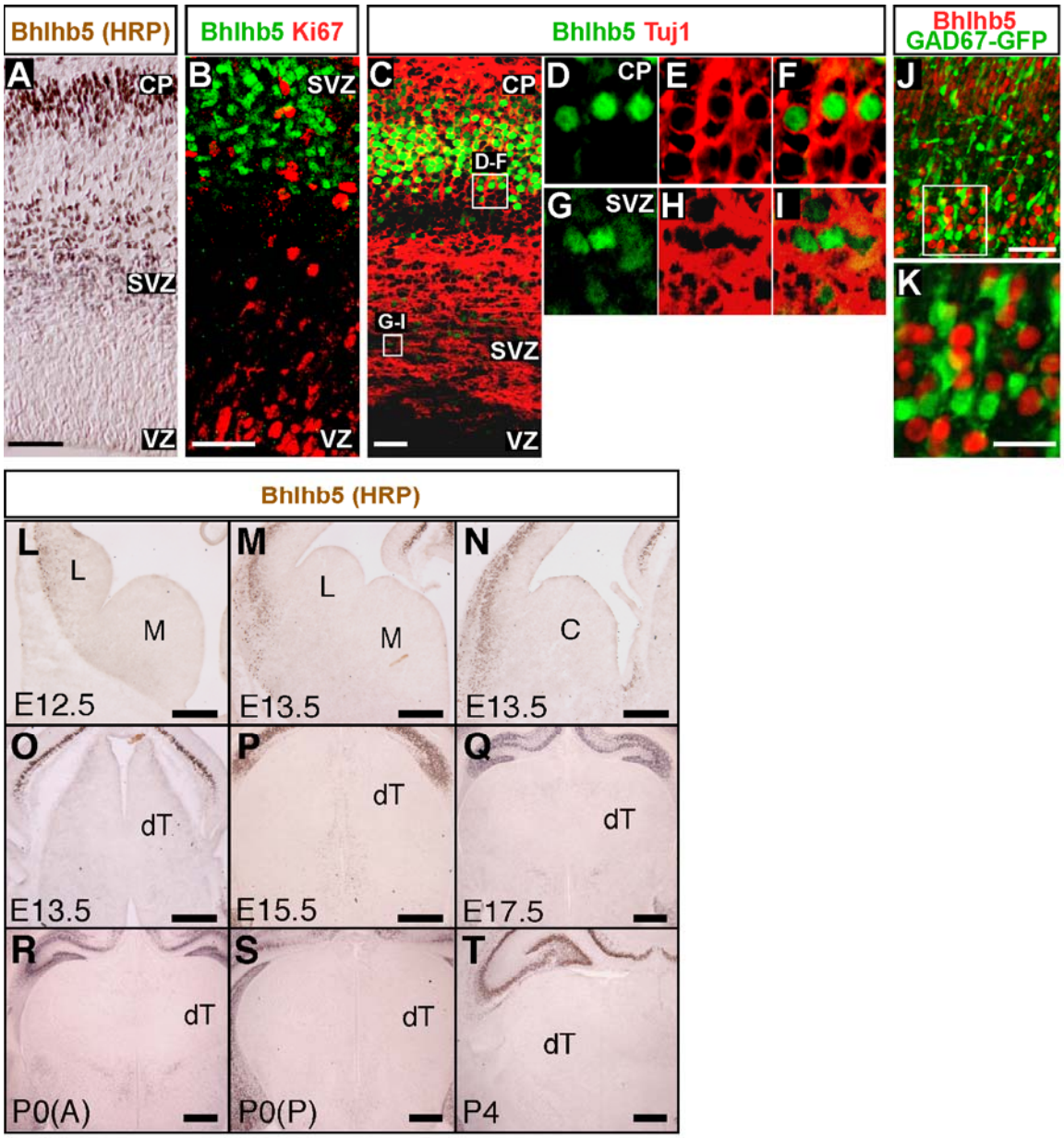
Bhlhb5 (HRP)
Bhlhb5 Ki67
Bhlhb5 Tuj1
Bhlhb5 GAD67-GFP
A
CP
SVZ
VZ
B
SVZ
VZ
C
CP
D-F
G-I
SVZ
VZ
D
CP
E
F
G
SVZ
H
I
J
K
Bhlhb5 (HRP)
L
L
M
E12.5
M
L
M
E13.5
N
C
E13.5
O
dT
E13.5
P
dT
E15.5
Q
dT
E17.5
R
dT
P0(A)
S
dT
P0(P)
T
dT
P4

Figure S2

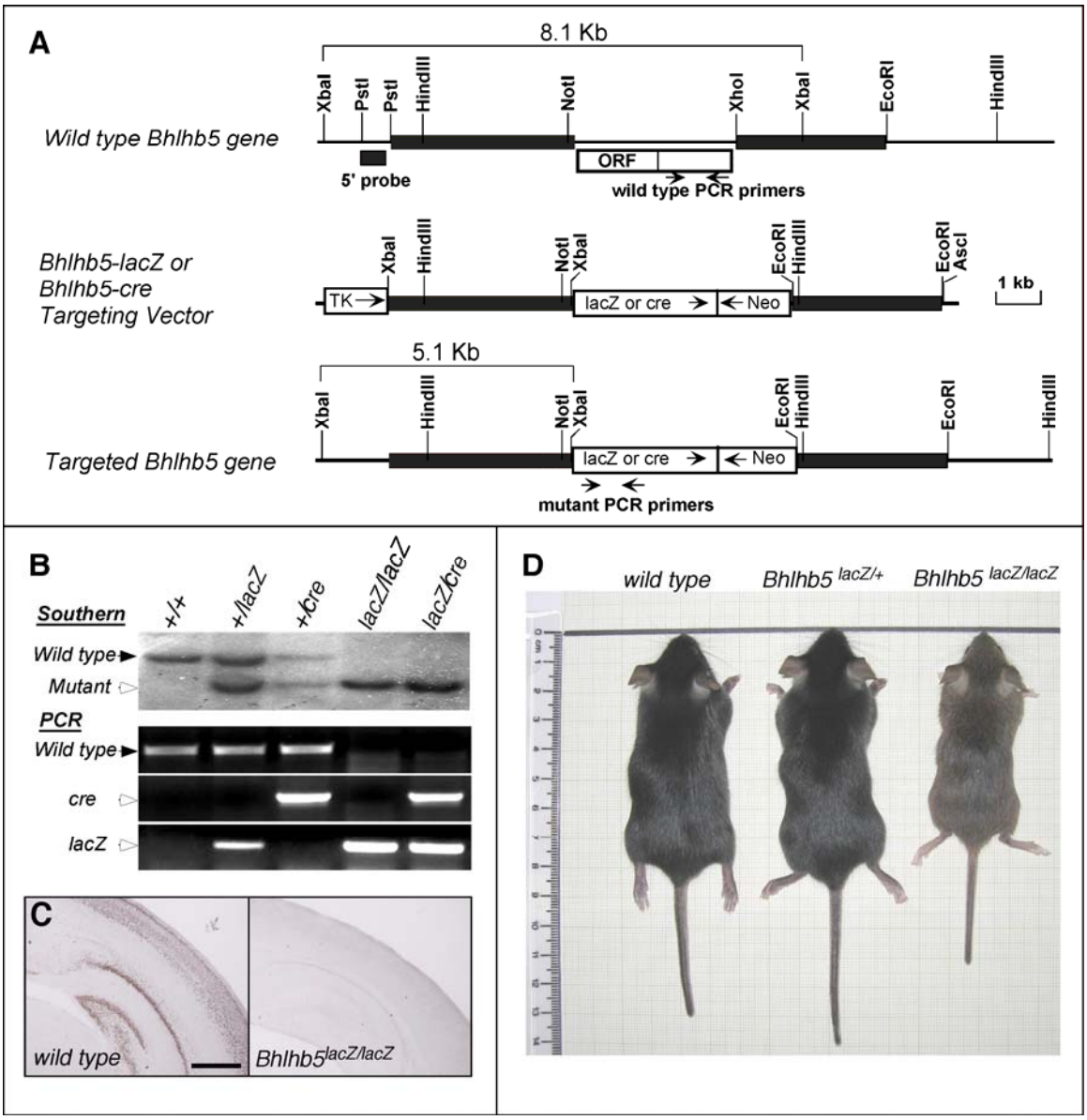
A
8.1 Kb
XbaI
PstI
PstI
HindIII
NotI
XhoI
XbaI
EcoRI
HindIII
Wild type Bhlhb5 gene
5' probe
ORF
wild type PCR primers
Bhlhb5-lacZ or
Bhlhb5-cre
Targeting Vector
XbaI
HindIII
NotI
XbaI
EcoRI
HindIII
EcoRI
AscI
TK
lacZ or cre
Neo
1 kb
5.1 Kb
XbaI
HindIII
NotI
XbaI
EcoRI
HindIII
EcoRI
HindIII
Targeted Bhlhb5 gene
lacZ or cre
Neo
mutant PCR primers
B
Southern
+/+
+/lacZ
+/cre
lacZ/lacZ
lacZ/cre
Wild type
Mutant
PCR
Wild type
cre
lacZ
C
wild type
Bhlhb5lacZ/lacZ
D
wild type
Bhlhb5 lacZ/+
Bhlhb5 lacZ/lacZ

Figure S3

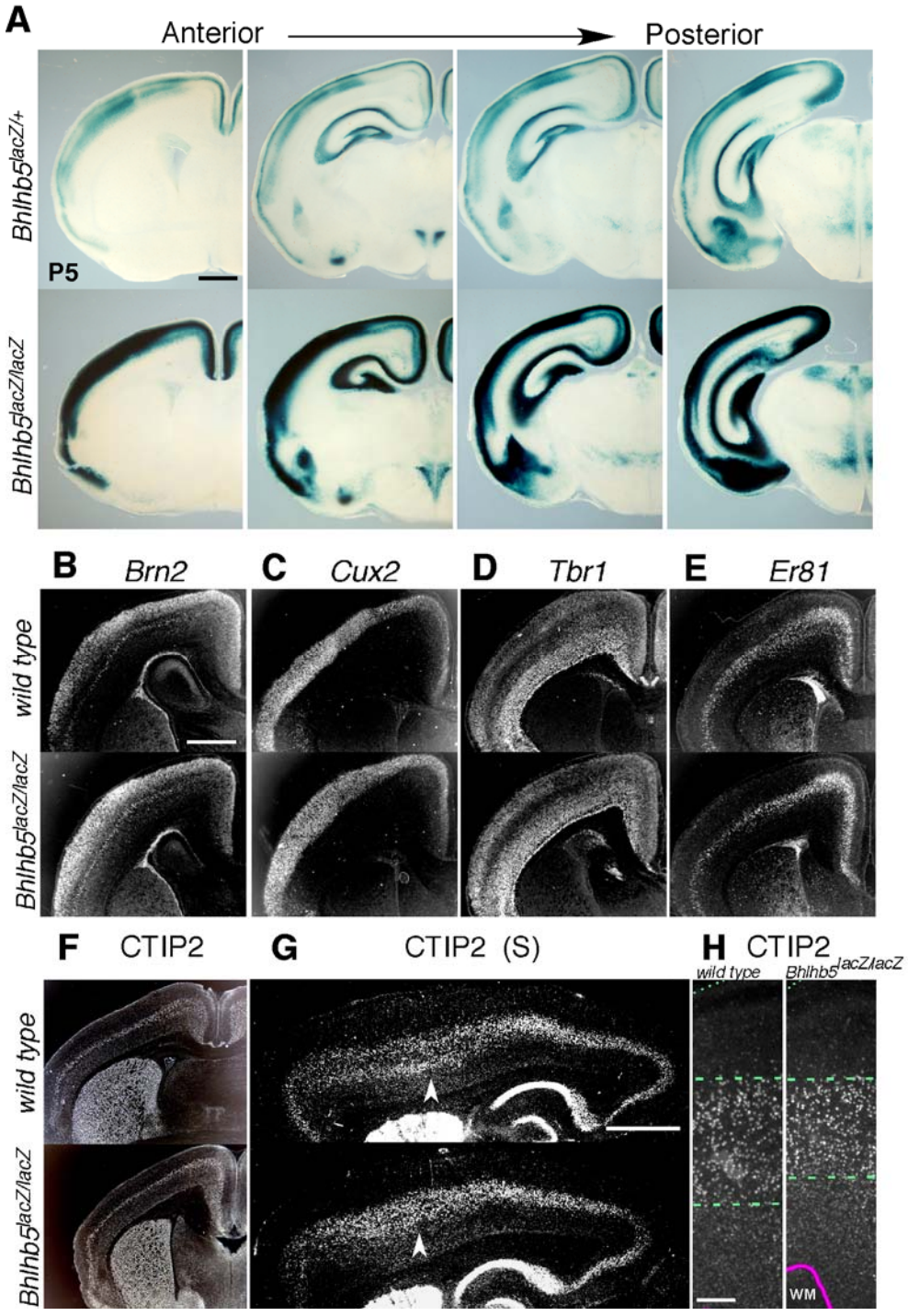
A
Anterior
Posterior
Bhlhb5lacZ/+
P5
Bhlhb5lacZ/lacZ
B Brn2
C Cux2
D Tbr1
E Er81
wild type
Bhlhb5lacZ/lacZ
F CTIP2
G CTIP2 (S)
H CTIP2
wild type
Bhlhb5lacZ/lacZ
WM

Figure S4

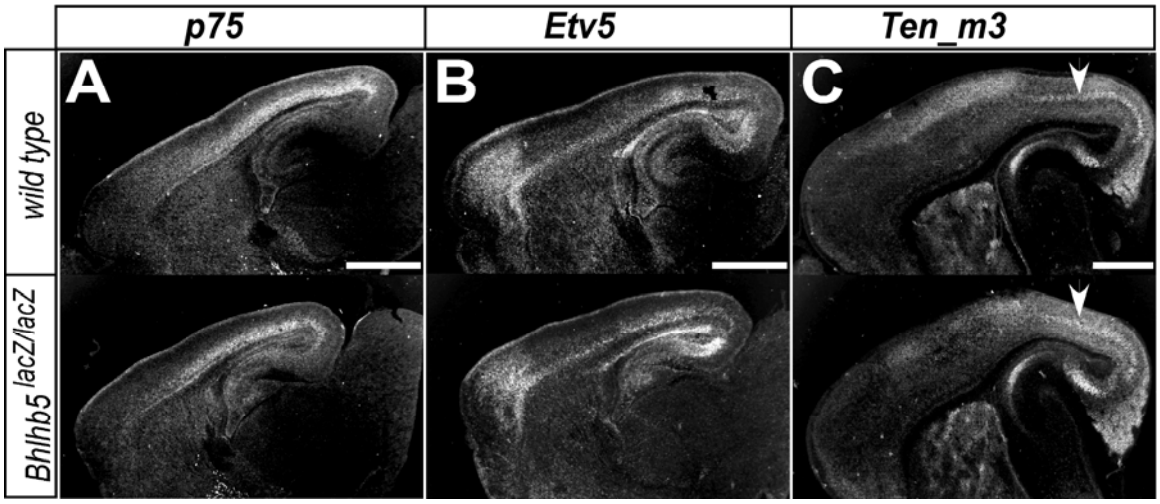

Figure S5

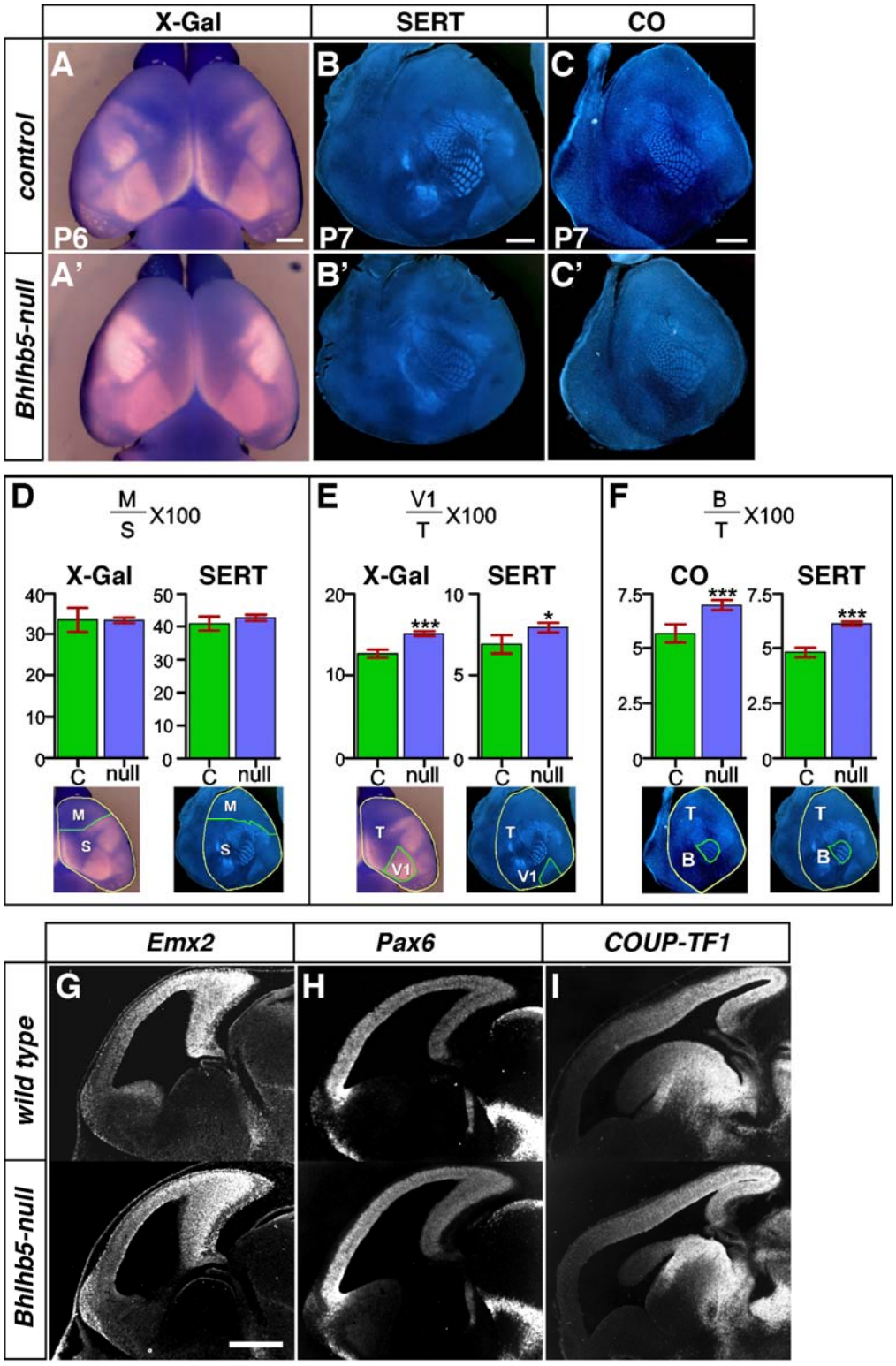
X-Gal
SERT
CO
control
Bhlhb5-null
A
B
C
A'
B'
C'
P6
P7
P7
D
M/S X100
E
V1/T X100
F
B/T X100
X-Gal
SERT
CO
SERT
C
null
M
S
T
V1
B
***
*
Emx2
Pax6
COUP-TF1
G
H
I
wild type
Bhlhb5-null

Figure S6

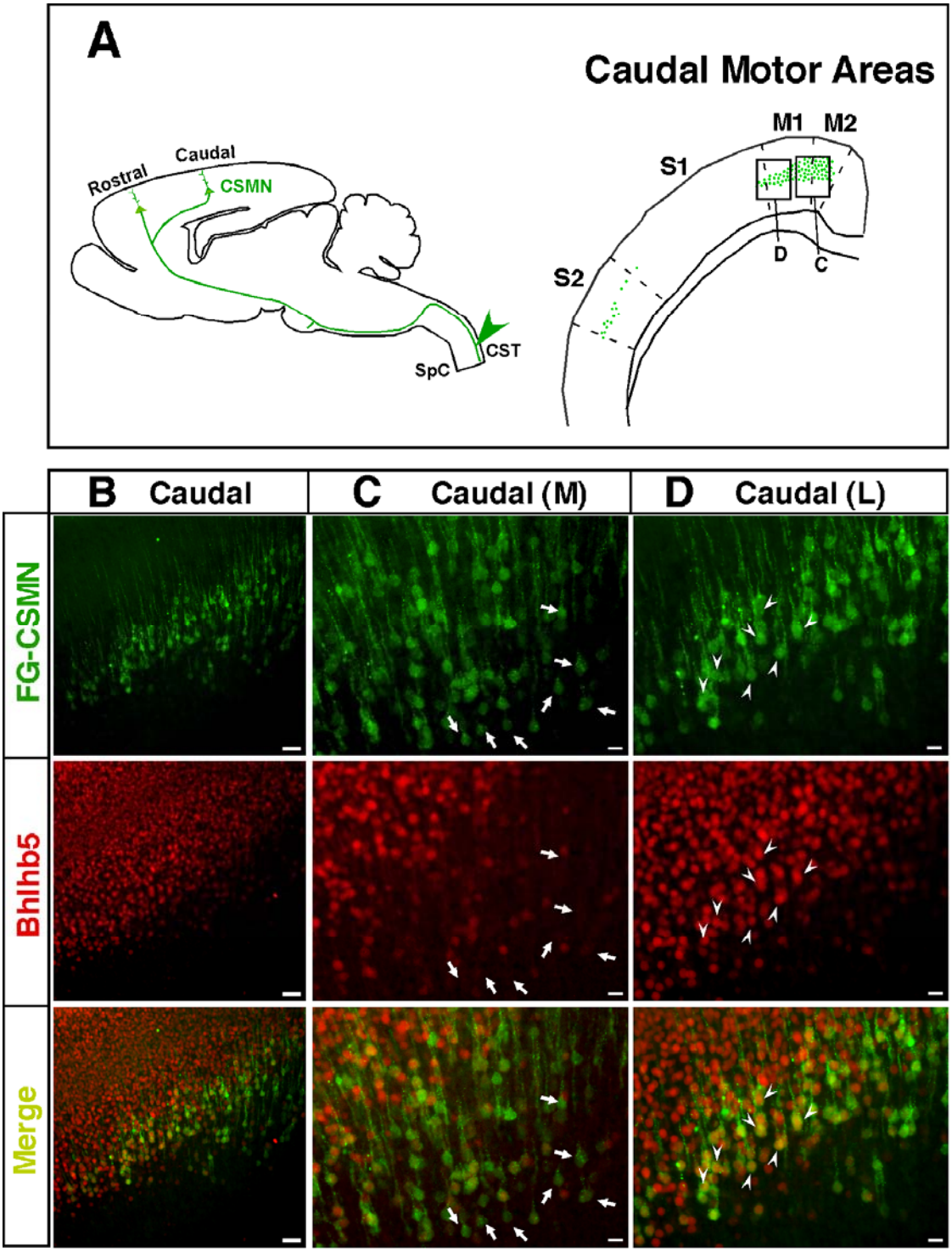
A
Caudal Motor Areas
Rostral
Caudal
CSMN
SpC
CST
M1
M2
S1
S2
D
C
B Caudal
C Caudal (M)
D Caudal (L)
FG-CSMN
Bhlhb5
Merge

Figure S7

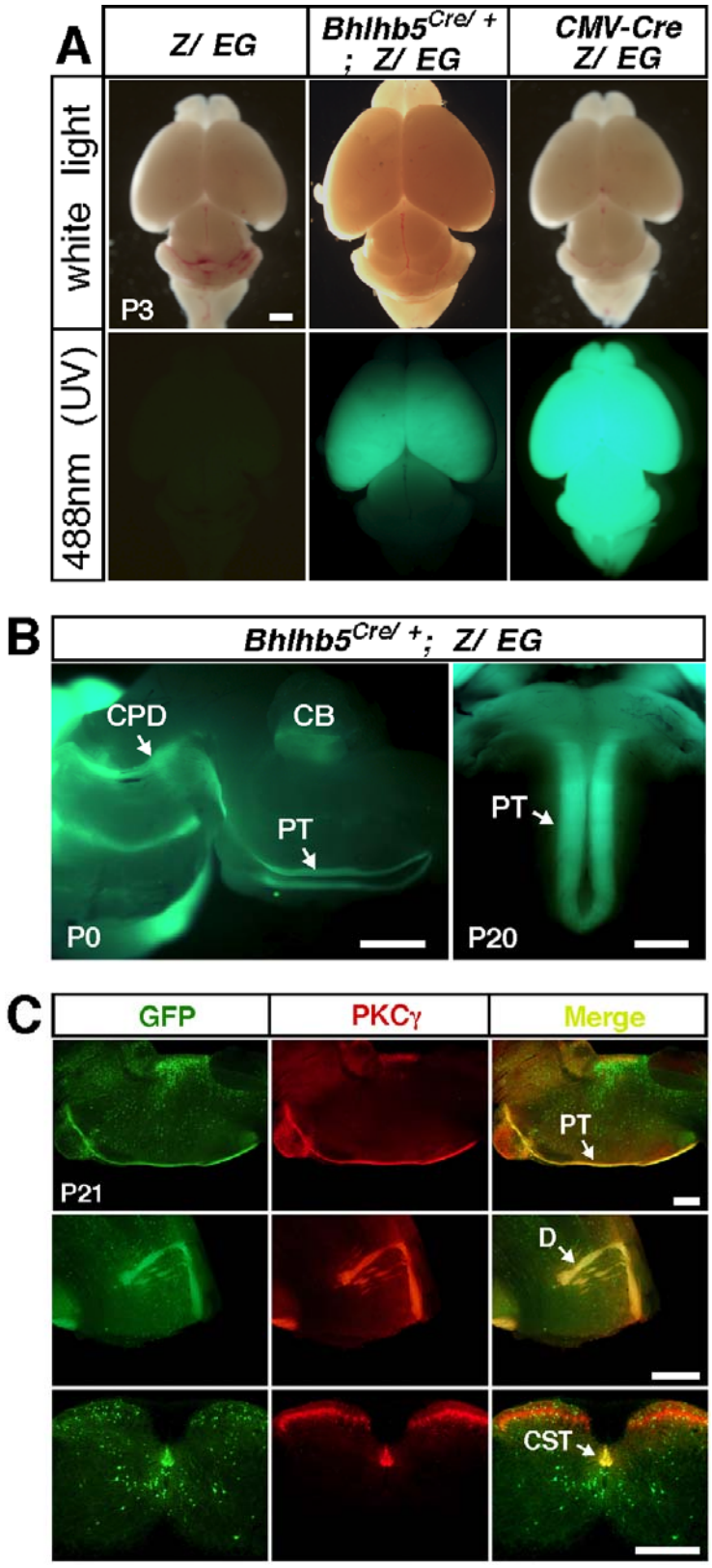
A
Z/ EG
Bhlhb5Cre/ + ; Z/ EG
CMV-Cre Z/ EG
white light
488nm (UV)
P3
B
Bhlhb5Cre/ +; Z/ EG
CPD
CB
PT
P0
PT
P20
C
GFP
PKCγ
Merge
P21
PT
D
CST

Figure S8

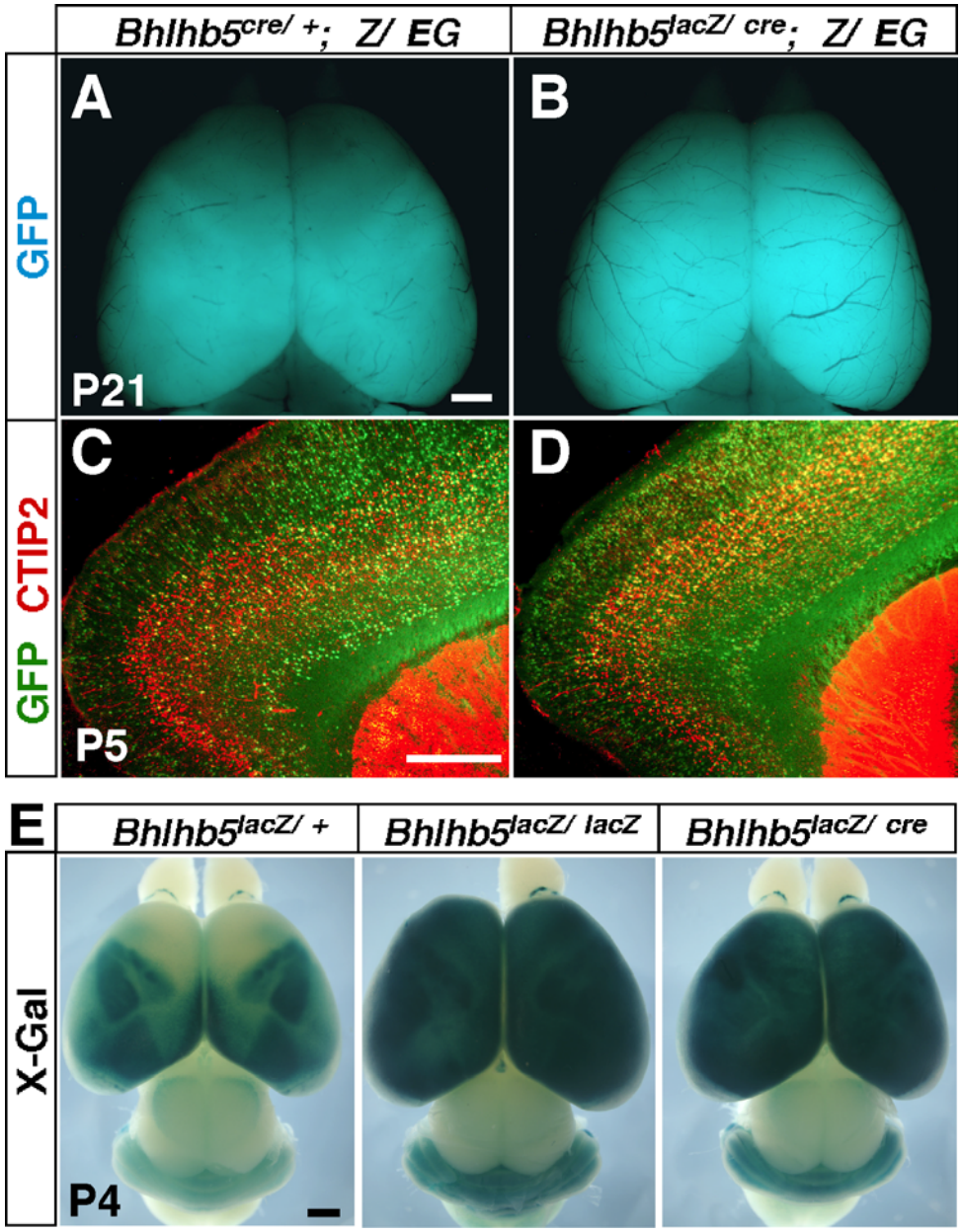
Bhlhb5cre/ +; Z/ EG
Bhlhb5lacZ/ cre; Z/ EG
A
B
GFP
P21
C
D
GFP CTIP2
P5
E
Bhlhb5lacZ/ +
Bhlhb5lacZ/ lacZ
Bhlhb5lacZ/ cre
X-Gal
P4

Table S1. Summary of Phenotypes Observed in *Bhlhb5* nulls

Table S1.1. Summary of Molecular Changes Observed in the Neocortex of *Bhlhb5* null *(Bhlhb5$^{lacZ/lacZ}$)* Mice

For each gene analyzed, *wild-types* n=3; *Bhlhb5* nulls n=3.

Gene	Age	Change Observed in *Bhlhb5* nulls
Cadherin 8	P3	Ectopic expression in layers II/III of the somatosensory cortex.
COUP-TF1	P5	Lack of expression in layer IV of the somatosensory cortex.
ephrin-A5	P3	Reduced expression in layers IV/V of the somatosensory cortex.
Lmo4	P5	Lack of expression in layer IV of the somatosensory cortex.
RORß	P3	Lack of expression in layer IV of caudal motor cortex.
Id2	P3	Lack of expression in layer V of caudal motor cortex.
EphA7	P3	Lack of expression in layer IV of the occipital cortex.
S100A10	P5	Reduced expression in Layer V of caudal motor cortex.
mu-crystallin	P5	Reduced expression in Layer V of caudal motor cortex.
Crim1	P5	Reduced expression in Layer V of caudal motor cortex.

Table S1.2. Summary of Cortical Map Analysis in *Bhlhb5* null Mice

			% change in *Bhlhb5* nulls compared with controls		
Method	**Genotype**	**n**	**Mx100/S**	**V1x100/T**	**Bx100/T**
X-Gal	*Bhlhb5$^{lacZ/+}$*	6			
X-Gal	*Bhlhb5$^{lacZ/lacZ}$*	5	— (p=0.96)	20% increase (p<0.0001)	
SERT	*wild-type*	7			
SERT	*Bhlhb5$^{lacZ/lacZ}$*	7	— (p=0.16)	14% increase (p=0.04)	26% increase (p<0.0001)
Cytochrome oxidase	*wild-type*	7			
Cytochrome oxidase	*Bhlhb5$^{lacZ/lacZ}$*	6			23% increase (p<0.0001)

SERT, serotonin transporter; M, rostral motor domain area; S, sensory domain area; V1, Primary visual area; B, Posteromedial barrel subfield area; T, Total cortical area; —, no change.

Table S1.3. Analysis of the Corticospinal Tract in *Bhlhb5* null Mice
Method: Anterograde tracing of corticospinal tract.

Injection site	Genotype	n	Age	Internal Capsule	Cerebral Peduncle	Pons	Ventral Medulla	Pyramidal decussation	Spinal Cord
Rostral	*wild-type*	4	P10	+	+	+	+	+	+
Rostral	*Bhlhb5$^{lacZ/lacZ}$*	4	P10	+	+	+	+	+	—
Caudal	*wild-type*	3	P10	+	+	+	+	+	+
Caudal	*Bhlhb5$^{lacZ/lacZ}$*	2	P10	+	+	+	—	—	—
Caudal	*Bhlhb5$^{lacZ/lacZ}$*	1	P10	+	+	+	+ Negligible	—	—

+, presence of DiI labeled fibers; —, absence of DiI labeled fibers.

Method: Bhlhb5 lineage tracing.

Genotype	n	Age	Internal Capsule	Cerebral Peduncle	Pons	Ventral Medulla	Pyramidal decussation	Spinal Cord
Bhlhb5$^{cre/+}$; Z/EG/+ (het)	4	P0	+	+	+	+	+	—
Bhlhb5$^{cre/lacZ}$; Z/EG/+ (null)	10	P0	+	+	+	—	—	—
Bhlhb5$^{cre/+}$; Z/EG/+ (het)	6	>P14	+	+	+	+	+	+
Bhlhb5$^{cre/lacZ}$; Z/EG/+ (null)	17	>P14	+	+	+	+ Reduced	+ Reduced	—

+, presence of *Bhlhb5*+ (GFP) fibers; —, absence of *Bhlhb5*+ (GFP) fibers.

Supplemental References

Feng, L., Xie, X., Joshi, P. S., Yang, Z., Shibasaki, K., Chow, R. L., and Gan, L. (2006). Requirement for Bhlhb5 in the specification of amacrine and cone bipolar subtypes in mouse retina. Development *133*, 4815-4825.

Gan, L., Wang, S. W., Huang, Z., and Klein, W. H. (1999). POU domain factor Brn-3b is essential for retinal ganglion cell differentiation and survival but not for initial cell fate specification. Dev Biol *210*, 469-480.

Gan, L., Xiang, M., Zhou, L., Wagner, D. S., Klein, W. H., and Nathans, J. (1996). POU domain factor Brn-3b is required for the development of a large set of retinal ganglion cells. Proc Natl Acad Sci USA *93*, 3920-3925.

Hevner, R. F., Daza, R. A., Rubenstein, J. L., Stunnenberg, H., Olavarria, J. F., and Englund, C. (2003). Beyond laminar fate: toward a molecular classification of cortical projection/pyramidal neurons. Dev Neurosci *25*, 139-151.

McEvilly, R. J., de Diaz, M. O., Schonemann, M. D., Hooshmand, F., and Rosenfeld, M. G. (2002). Transcriptional regulation of cortical neuron migration by POU domain factors. Science *295*, 1528-1532.

Nieto, M., Monuki, E. S., Tang, H., Imitola, J., Haubst, N., Khoury, S. J., Cunningham, J., Gotz, M., and Walsh, C. A. (2004). Expression of Cux-1 and Cux-2 in the subventricular zone and upper layers II-IV of the cerebral cortex. J Comp Neurol *479*, 168-180.

Sugitani, Y., Nakai, S., Minowa, O., Nishi, M., Jishage, K., Kawano, H., Mori, K., Ogawa, M., and Noda, T. (2002). Brn-1 and Brn-2 share crucial roles in the production and positioning of mouse neocortical neurons. Genes Dev *16*, 1760-1765.

Zimmer, C., Tiveron, M. C., Bodmer, R., and Cremer, H. (2004). Dynamics of Cux2 expression suggests that an early pool of SVZ precursors is fated to become upper cortical layer neurons. Cereb Cortex *14*, 1408-1420.